THE JOURNAL OF BIOLOGICAL CHEMISTRY
Vol. 277, No. 11, Issue of March 15, pp. 9580–9589, 2002
Printed in U.S.A.

Members of the Zyxin Family of LIM Proteins Interact with Members of the p130^{Cas} Family of Signal Transducers*

Received for publication, June 23, 2001, and in revised form, December 20, 2001
Published, JBC Papers in Press, January 8, 2002, DOI 10.1074/jbc.M106922200

Jinseong Yi, Susanne Kloeker, Christopher C. Jensen, Susanne Bockholt, Hiroaki Honda‡, Hisamura Hirai‡, and Mary C. Beckerle§

From the Huntsman Cancer Institute and Department of Biology, University of Utah, Salt Lake City, Utah 84112 and the ‡University of Tokyo, 7-3-1, Hongo, Bunkyo-ku, Tokyo, 113-8655, Japan

Integrin binding to extracellular matrix proteins induces formation of signaling complexes at focal adhesions. Zyxin co-localizes with integrins at sites of cell-substratum adhesion and is postulated to serve as a docking site for the assembly of multimeric protein complexes involved in regulating cell motility. Recently, we identified a new member of the zyxin family called TRIP6. TRIP6 is localized at focal adhesions and overexpression of TRIP6 slows cell migration. In an effort to define the molecular mechanism by which TRIP6 affects cell migration, the yeast two-hybrid assay was employed to identify proteins that directly bind to TRIP6. This assay revealed that both TRIP6 and zyxin interact with CasL/HEF1, a member of the Cas family. This association is mediated by the LIM region of the zyxin family members and the SH2 domain-binding region of CasL/HEF1. Furthermore, the association between p130^{Cas} and the two zyxin family members was demonstrated to occur *in vivo* by co-immunoprecipitation. Zyxin and Cas family members may cooperate to regulate cell motility.

Integrin-mediated cell adhesion to extracellular matrix (ECM)[1] components is crucial for many cell activities including cell survival, proliferation, migration, and differentiation (1–5). Upon binding to the substratum, integrins recruit many cytoskeletal components to the sites of cell adhesion and establish a structural link between the elements of the ECM and actin filaments. In addition to contributing to the physical link between the extracellular and intracellular environments, integrin engagement also regulates several signaling pathways (2, 6, 7). Although the cytoplasmic domains of integrins do not exhibit any enzymatic activity, they can activate intracellular signaling pathways by recruiting a number of signaling proteins to focal adhesions (8–10).

Recent studies have identified a number of proteins that participate in integrin-dependent signaling pathways (10–13). These signaling molecules include non-receptor tyrosine kinases (14, 15), serine/threonine kinases (7, 16–18), a lipid kinase (19), protein-tyrosine phosphatases (20–24), and small GTPases in the Ras and Rho families (25–29). In addition to proteins that harbor catalytic domains, integrins recruit several adaptor proteins that facilitate the assembly of multicomponent signaling complexes (30–32). For instance, upon substratum adhesion, the adaptor protein p130^{Cas} (p130$^{Crk\text{-}associated\ substrate}$) is recruited to integrin-rich sites where it docks several regulatory molecules including Src, Crk, and FAK (focal adhesion kinase) (33–35).

Members of the zyxin family have also been postulated to function in integrin-mediated signaling (36). Zyxin, the founding member of the family, is a phosphoprotein that is localized at focal adhesions and along actin filaments (37, 38). The protein displays an NH_2-terminal proline-rich region, one or more leucine-rich nuclear export signals (depending on the species) and three copies of the LIM motif at its COOH terminus (Fig. 1*A*) (36, 39, 40). The NH_2-terminal proline-rich region of zyxin displays four proline-rich repeats that serve as docking sites for Mena (mammalian Ena) and VASP (vasodilator-activated phosphoprotein) (36, 41, 42), proteins that are postulated to play an important role in the assembly and dynamics of actin filaments (42–44). Sequences in the NH_2 terminus of zyxin also provide a docking site for the actin-bundling protein, α-actinin (45–47), further bolstering a link between zyxin and elements of the actin cytoskeleton. Consistent with the possibility that zyxin plays some role in the regulation of the actin cytoskeleton, targeting of zyxin to the inner leaflet of the plasma membrane or mitochondria stimulates actin assembly (48, 49). As is the case for the proline-rich sequences in the NH_2 terminus of zyxin, the COOH-terminal LIM domains of zyxin are predicted to mediate a series of protein-protein interactions (40, 50). Thus far, two protein binding partners for the triplet LIM series in zyxin have been identified. The most NH_2-terminal LIM domain (LIM1) of zyxin interacts with members of the cysteine-rich protein family that play important roles in muscle (40, 51). A second binding partner of the LIM domains, the serine/threonine kinase h-warts/LATS1, was recently reported to interact with LIM1–2 of zyxin during mitosis (52). H-wart/LATS1 is a component of mitotic apparatus and negatively regulates Cdc2 activity (52). Evidence of an association between zyxin and a regulator of mitotic progression is consistent with the postulated role of zyxin in signaling. Moreover, although zyxin is found at focal adhesions and faintly in the leading edge, it also has the capacity to shuttle between the cytoplasm and the nucleus (36, 39), raising the possibility that zyxin may relay information between these two compartments.

* This work was supported by National Institutes of Health Grant GM50877 (to M. C. B.), National Research Service Awards (to S. K. and S. B.), the Huntsman Cancer Foundation, and the University of Utah DNA-Peptide Facility and Sequencing Facility technical support Grant CA42014. The costs of publication of this article were defrayed in part by the payment of page charges. This article must therefore be hereby marked "*advertisement*" in accordance with 18 U.S.C. Section 1734 solely to indicate this fact.

§ To whom correspondence should be addressed: Huntsman Cancer Institute, 2000 Circle of Hope, University of Utah, Salt Lake City, UT 84112. Tel.: 801-581-4485; Fax: 801-581-2175; E-mail: mary.beckerle@hci.utah.edu.

[1] The abbreviations used are: ECM, extracellular matrix; Cas, Crk-associated substrate; FAK, focal adhesion kinase; PBS, phosphate-buffered saline; DMEM, Dulbecco's modified Eagle's medium; X-gal, 5-bromo-4-chloro-3-indolyl β-D-galactopyranoside; LPP, lipoma-preferred partner; SH3, Src homology domain 3; TRIP6, thyroid receptor interacting protein 6.

Several years ago, a cDNA sequence that encoded two LIM domains with a high degree of similarity to those in zyxin was identified in a screen for proteins that interacted with the thyroid hormone receptor (53). Although the physiological significance of the interaction between the thyroid hormone receptor and TRIP6 (thyroid receptor interacting protein 6) has yet to be confirmed, we became interested in the protein because of its potential relationship to zyxin. Further characterization of TRIP6 revealed a similar domain structure to that of zyxin (54). Additionally, the subcellular distribution of exogenous TRIP6 was comparable with zyxin (55). These observations suggest that TRIP6 is a member of the zyxin family.

In an effort to learn more about the function of TRIP6 and its relationship to zyxin, we examined the subcellular distribution of endogenous TRIP6, studied the effect of TRIP6 overexpression on cell migration, and performed a two-hybrid screen to identify potential TRIP6-binding partners. Here we report that both TRIP6 and zyxin interact with $p130^{Cas}$ and CasL/HEF1, two members of the Cas family. Cas family members, $p130^{Cas}$ (56), CasL/HEF1 (human enhancer of filamentation 1 (57, 58)), and Efs/Sin (embryonal Fyn-associated substrate/Src interacting protein (59, 60)), are adaptor proteins that play a role in cell motility. Co-expression of $p130^{Cas}$ and FAK in Chinese hamster ovary cells increases cell migration as compared with FAK expression alone (61). Cell migration is also enhanced by co-expression of $p130^{Cas}$ and Crk (62). This Cas-Crk mediated stimulation of cell migration is blocked by expression of $p130^{Cas}$ lacking the Crk-binding site or by expression of Crk lacking a functional SH2 domain. Targeted gene disruption studies have also demonstrated that Cas is involved in the regulation of cell locomotion (63, 64). The assembly of signaling complexes involving Cas family members has been shown to be crucial for normal cellular responses to integrin engagement (65). The demonstration that zyxin and Cas family members are present in the same molecular complex provides a direct connection between zyxin family members and Cas-dependent motility.

MATERIALS AND METHODS

Antibody Preparation

Anti-TRIP6 antibody was generated in New Zealand White rabbits against a peptide sequence deduced from TRIP6 cDNA sequence analysis (54). The amino acid sequence ^{10}KQPEPARAPQGRAIPR^{25} conjugated to maleimide-activated keyhole limpet hemocyanin (Pierce) was immunized three times by subcutaneous injections and subsequent intravenous injections at 4-week intervals. The anti-TRIP6 antiserum was affinity purified using the immunogen peptide linked to Sulfolink gel (Pierce) according to a method described elsewhere (66). Briefly, the polyclonal antiserum diluted 1:10 in 10 mM Tris, pH 7.5, was passed through the column, washed extensively with 10 mM Tris, pH 7.5, and the bound antibodies were eluted with 100 mM glycine, pH 2.5. Fractions were collected in tubes containing 1 M Tris, pH 8. The antiserum was characterized by immunoblotting and immunoprecipitation of [^{35}S]methionine/cysteine-labeled IMR-90 cell lysates prepared under denaturing conditions.

Cell Labeling and Immunoprecipitation

IMR-90 cells were radiolabeled with [^{35}S]methionine/cysteine (Tran^{35}S-label; ICN Biochemicals Inc.) for immunoprecipitation under denaturing conditions. Metabolic labeling of cells was carried out as described elsewhere (67). Metabolically labeled cells were washed three times with PBS, lysed in 250 μl of Laemmli sample buffer with protease inhibitors (0.1 mM phenylmethylsulfonyl fluoride, 0.1 mM benzamidine, 1 μg/ml pepstatin A, 1 μg/ml phenanthroline) and scraped from the dishes. Cell lysates were boiled for 5 min to denature the proteins and centrifuged at 12,000 $\times$ *g* for 10 min. Immunoprecipitation was carried out after dilution of the supernatants in 4 volumes of modified RIPA buffer without SDS (50 mM Tris, pH 7.6, 150 mM NaCl, 1% Triton X-100, 0.5% sodium deoxycholate) supplemented with protease inhibitors. The lysates were precleared with protein A-agarose beads. The precleared lysates were then incubated for 1.5 h at 4 °C with either 5 μl of anti-TRIP6 antiserum or 5 μl of corresponding preimmune serum and further incubated for 1 h with protein A-agarose beads. The beads were washed four times with modified RIPA buffer containing 0.2% SDS and boiled for 5 min in 2 $\times$ Laemmli sample buffer. The immunoprecipitates were resolved on 12.5% SDS-polyacrylamide gels. The gels were dried and subjected to autoradiography.

For co-immunoprecipitation of interacting proteins from adherent cell lysates, IMR-90 cells grown on tissue culture dishes in DME supplemented with 10% fetal bovine serum were washed two times with PBS and lysed in buffer A (50 mM Tris, pH 7.6, 150 mM NaCl, 1% Triton X-100, 0.02% SDS, 0.5 mM EDTA, protease inhibitors). After incubation on ice for 30 min, the lysates were centrifuged at 10,000 $\times$ *g* for 15 min and the soluble fractions were recovered for immunoprecipitation. Lysates from non-adherent cells were prepared as described elsewhere with a slight modification (68). Briefly, adherent cells were detached by trypsinization and washed twice with DME containing 1% fetal bovine serum. Detached cells were held in suspension for 1 h at 37 °C. Cells were then collected by centrifugation, washed twice with Hanks' balanced salt solution and then lysed in buffer A. The lysates were centrifuged at 12,000 $\times$ *g* for 10 min and supernatants were collected for immunoprecipitation. The lysates were incubated with protein A-agarose beads for 1 h at 4 °C and precleared supernatants were collected after centrifugation. For the zyxin immunoprecipitation, precleared lysates containing 0.5 mg of protein were incubated for 2 h at 4 °C with 5 μl of zyxin-specific antisera or preimmune sera. For the TRIP6 immunoprecipitation, 1.0 mg of precleared lysates were similarly incubated with 40 μl of affinity-purified TRIP6 antibody or rabbit IgG as a negative control. Protein A-agarose beads were added to the mixture and incubated for an additional hour. The beads were washed four times with 1 ml of buffer A and the immunoprecipitates were eluted by boiling the beads in 2 $\times$ Laemmli sample buffer for 5 min. The immunoprecipitates were resolved on 7.5 or 12.5% SDS-polyacrylamide gel and transferred onto nitrocellulose paper for immunoblotting. Zyxin and $p130^{Cas}$ were detected by the enhanced chemiluminescence detection method using horseradish peroxidase-linked goat anti-rabbit or anti-mouse immunoglobulins as a secondary reagent (Amersham Biosciences, Inc.). The blots were then stripped in stripping solution (100 mM 2-mercaptoethanol, 2% SDS, 62.5 mM Tris, pH 6.8) for 1 h at 50 °C and washed three times in TBS, 0.1% Tween. After stripping, the blots were reprobed with anti-vinculin antibody (Sigma) and developed using enhanced chemiluminescence.

Immunofluorescence

Indirect immunofluorescence was performed as described previously (69). Briefly, cells were grown on glass coverslips coated with 100 μg/ml fibronectin (Invitrogen) in DME supplemented with 10% fetal bovine serum. Coverslips were washed in PBS, fixed for 15 min with 3.7% formaldehyde in PBS, and permeabilized for 4 min with 0.2% Triton X-100 in PBS. After washing in Tris-buffered saline (TBS: 50 mM Tris, pH 7.6, 150 mM NaCl), the coverslips were incubated with primary antibodies at 37 °C for 60 to 120 min, washed for 15 min in TBS, and subsequently incubated with fluorescein isothiocyanate- or Texas Red-conjugated secondary antibodies. The coverslips were mounted with gelvatol after washing for 15 min in TBS. Primary antibodies used in this study included the following: an affinity purified rabbit polyclonal anti-TRIP6 antibody B59, a rabbit polyclonal anti-zyxin antibody B38 (1:400), the anti-vinculin monoclonal antibody hVIN-1 (1:200; Sigma), monoclonal anti-FLAG antibody (1:600; Sigma), and a rabbit polyclonal anti-β-galactosidase antibody (1:1000; Cappel). Secondary antibodies included fluorescein isothiocyanate goat anti-mouse IgG (1:250), fluorescein isothiocyanate goat anti-rabbit IgG (1:500; Cappel), and Texas Red-goat anti-mouse IgG (1:200; Molecular Probes). Cell images were visualized on a Zeiss Axiophot microscope.

Expression Plasmid Construction

The 5′ end of the human TRIP6 sequence was used to search the expressed sequence tag data base with the BLAST protocol. One highly homologous murine cDNA clone (W58878) was obtained from Genome Systems (St. Louis, MO) and sequenced in its entirety. A FLAG epitope was engineered on the amino terminus of TRIP6 and subsequently subcloned into the *Eco*RI and *Not*I sites of the pcDNA3.1 vector (Invitrogen). The construct was verified by DNA sequencing.

Transient Transfection of 10T1/2 Cells

Mouse fibroblasts (10T1/2) were plated at 3.0 $\times$ 10^5 cells/60-mm dish ~22 h prior to transfection. The cells were co-transfected with 0.5 μg of a reporter construct encoding β-galactosidase and 2 μg of empty expres-

sion vector or vector containing FLAG-TRIP6 cDNA. The transient transfection was performed using LipofectAMINE Plus (16 μl Plus reagent and 10 μl of LipofectAMINE, Invitrogen) and cells were allowed to incorporate cDNA constructs for 4 h. Forty h post-transfection, cells were prepared for the cell migration assay or harvested in 2 × Laemmli sample buffer to examine TRIP6 expression by Western analysis. A polyclonal TRIP6 antibody directed against the murine sequence (CK-QPEPSRLPQGRSLPR) was utilized as the primary antibody. TRIP6 was visualized by the enhanced chemiluminescence detection method. The relative amount of TRIP6 expression was quantified by using the Kodak Image Station 440 CF and Kodak Digital Science 1D 3.0.2 software. Transfection efficiency was ~35% as measured by X-gal staining.

Haptotaxis Migration Assay

Haptotaxis migration assays were performed as previously described (62). Briefly, cell migration assays were executed using modified Boyden chambers (24-well cell culture inserts containing polyethylene terephthalate membranes, 8-μm pores). The underside of the membrane was coated overnight at 4 °C with bovine serum albumin or fibronectin (20 μg/ml). The inserts were rinsed one time with PBS and then placed into the lower chamber containing 750 μl of DMEM plus 10% fetal bovine serum. Cells were harvested with trypsin/EDTA, washed twice using serum-free DMEM, and resuspended to 5.0×10^5 cells/ml. Approximately 125,000 cells were added to the top of each migration chamber and allowed to migrate to the underside of the membrane for 6 h at 37 °C, 5% CO_2. Nonmigratory cells on the upper surface of the membrane were mechanically removed with a cotton swab. Cells attached to the underside of the membrane were stained with X-gal substrate. Stained cells were photographed and counted (per field) with an inverted phase-contrast microscope using a ×10 objective. Background migration was determined by counting the number of β-galactosidase-expressing cells migrating on bovine serum albumin. These values were subtracted from the number of transfected cells migrating on fibronectin. Each determination represents the average of three individual wells and error bars represent the standard error of the mean.

Yeast Two-hybrid Screen

Strains, Plasmids, and Library—The *Saccharomyces cerevisiae* reporter strain L40 (*MATa his3–200 trp1–901 leu2–3,112 ade2 lys2–801am URA3::(lexAop)8-lacZ LYS2::(lexAop)4-HIS3* (70)) was used for screening and measurement of reporter gene expression. The yeast strain DY151 (also known as W303-1B, *MATα ade2-1 can1–100 his3–11 leu2-3 trp1-1 ura3-1*; (71)) was used in mating assays and to perform specificity test. The prey plasmid pVP16 and mouse embryo cDNA library cloned into pVP16 have been described elsewhere (70). pVP16 contains a selectable marker *LEU2*. The bait vector plasmid pBTM116/ADE2 that contains the *ADE2* gene and a selectable marker *TRP1* has been described elsewhere (72). The bait plasmid pBTM116/ADE2-TRIP6LIM(1–2) was constructed by subcloning a PCR-amplified DNA sequence encoding the first and second LIM domains of TRIP6 (amino acid residues 276–393) into *Eco*RI site of pBTM116/ADE2. Other bait constructs containing each individual LIM domain, LIM(1–2), LIM(2–3), and LIM(1–3) of human zyxin were constructed by subcloning into *Eco*RI site of pBTM116/ADE2. $p130^{Cas}$ DNA fragments (the full-length $p130^{Cas}$ cDNA was kindly provided by Dr. T. Parsons) encoding a part (amino acid residues 319–471) or all of the SH2 domain-binding substrate region (amino acid residues 212–525) of $p130^{Cas}$ were subcloned into the *Not*I site of pVP16 and *Bam*HI site of pBTM116/ADE2.

Library Screen—The yeast strain L40 was first transformed with pBTM116/ADE2-TRIP6LIM(1–2) and isolated on selective medium lacking tryptophan. The yeast strain was then transformed with mouse cDNA library by electroporation. An estimated 5×10^6 independent transformants were plated on medium lacking tryptophan, leucine, uracil, and histidine with 45 mM 3-aminotriazole to select for cells that transactivate the *HIS3* reporter gene. HIS+ clones were grown on medium lacking tryptophan and leucine for 2 days and then assayed for *lacZ* expression after the yeast cells were transferred onto nitrocellulose filter. HIS+/LacZ+ isolates were grown in tryptophan+/leucine− plates containing 10 mg/liter adenine to eliminate pBTM116/ADE2-TRIP6LIM(1–2) bait plasmid. Plasmid loss was confirmed by formation of red colonies and tryptophan auxotrophy. Resulting red and LEU+/TRP− isolates contain only prey plasmids. LEU+/TRP− isolates were assayed for *lacZ* expression. Yeast containing prey sequences that failed to activate *lacZ* in the absence of the bait were then mated with DY151 strain containing pBTM116/ADE2, pBTM116/ADE2-Lamin, or original bait plasmid pBTM116/ADE2-TRIP6LIM(1–2). The diploids were then assayed for activation of the *lacZ* reporter to eliminate prey clones that interact nonspecifically with LexA or LexA-Lamin. The prey sequences that specifically interact with the TRIP6LIM(1–2) were further tested for interaction with zyxinLIM sequences.

Quantitative β-Galactosidase Assay

To measure the relative strength of each two-hybrid interaction, a quantitative β-galactosidase assay was performed. Yeast strains were grown to stationary phase in selective medium lacking tryptophan and leucine. The cultures were diluted in 3 ml of fresh medium (A_{600} ~ 0.2) and then incubated with shaking until A_{600} reached 0.5–0.8. Cells were pelleted and resuspended in the same volume of Z-buffer (60 mM Na_2HPO_4, 40 mM NaH_2PO_4, 10 mM KCl, 1 mM $MgSO_4$, 40 mM β-mercaptoethanol). 50 μl of chloroform and 50 μl of 0.1% SDS were added and vortexed at maximum speed for 30 s. 0.2 ml of fresh *o*-nitrophenyl β-D-galactopyranoside solution (4 mg/ml in Z-buffer) was added and incubated at 30 °C. The reaction was stopped by adding 0.4 ml of 1 M Na_2CO_3 when a yellow color appeared (in 10 to 30 min) and the solution was centrifuged at 14,000 × *g* for 10 min. A_{420} of the supernatants was monitored and adjusted by timing 1.5 (initial culture volume: total assay volume). Specific β-galactosidase activity (Miller units) was calculated using the following formula: Miller units = $A_{420} \times 1000/(A_{600} \times$ incubation time (min) × culture volume (ml)).

RESULTS

Endogenous TRIP6 Is Targeted to Focal Adhesions—We have recently identified TRIP6 as a member of the zyxin family (54). To date, three members of the zyxin family have been identified: zyxin, the lipoma-preferred partner (LPP), and TRIP6 (Fig. 1*A*). As a first step to study the cellular function of TRIP6, polyclonal antibodies directed against amino acid residues 10–25 of human TRIP6 were produced. A Western immunoblot analysis shows that the anti-TRIP6 antiserum specifically recognizes a protein doublet with apparent molecular weights of 50,000 and 48,000 (Fig. 1*B*, *middle panel*). The calculated molecular weight of TRIP6 based on cDNA sequence analysis is 50,300. Similarly, this antiserum specifically immunoprecipitates a 48–50-kDa protein doublet from a lysate of [^{35}S]methionine/cysteine-labeled IMR-90 prepared under denaturing conditions (Fig. 1*B*, *right panel*). The 48–50-kDa doublet was not detected by Western immunoblot or immunoprecipitation when preimmune serum was used (Fig. 1*B*). No splice variants of TRIP6 have been identified and thus, the doublet may result from post-translational modification.

Epitope-tagged TRIP6 localizes at focal adhesions when expressed in mammalian cells (73). To confirm the subcellular localization of endogenous TRIP6, indirect immunofluorescence was carried out using an affinity purified antibody directed against TRIP6. TRIP6 is extensively co-localized with vinculin at focal adhesions in human fibroblasts (Fig. 1*C*). The subcellular distribution of TRIP6 resembles that of zyxin and LPP (37, 74).

Cells Overexpressing FLAG-TRIP6 Exhibit Reduced Cell Migration—Zyxin has been implicated in cell motility (46). To evaluate whether TRIP6 plays a role in cell migration, murine TRIP6 was expressed in mouse fibroblasts. Immunofluorescence analysis of transfected cells confirmed localization of epitope-tagged TRIP6 to focal adhesions (Fig. 2, *A* and *B*). The amount of TRIP6 protein was estimated to be ~5–10-fold higher in TRIP6-transfected cell lysates than in vector-transfected cell lysates (Fig. 2*C*) as determined by quantitative Western blot analysis with a murine-specific TRIP6 antibody. The effect of TRIP6 expression on migratory behavior was assayed using the haptotaxis migration assay (Fig. 2*D*). Transient overexpression of TRIP6 resulted in an ~50% decrease in the number of transfected migrating cells ($p = 0.035$) using fibronectin as the extracellular matrix. These findings provide further evidence that TRIP6 is involved in cellular movement; however, molecular interactions between TRIP6 and components of the migration machinery remained to be identified.

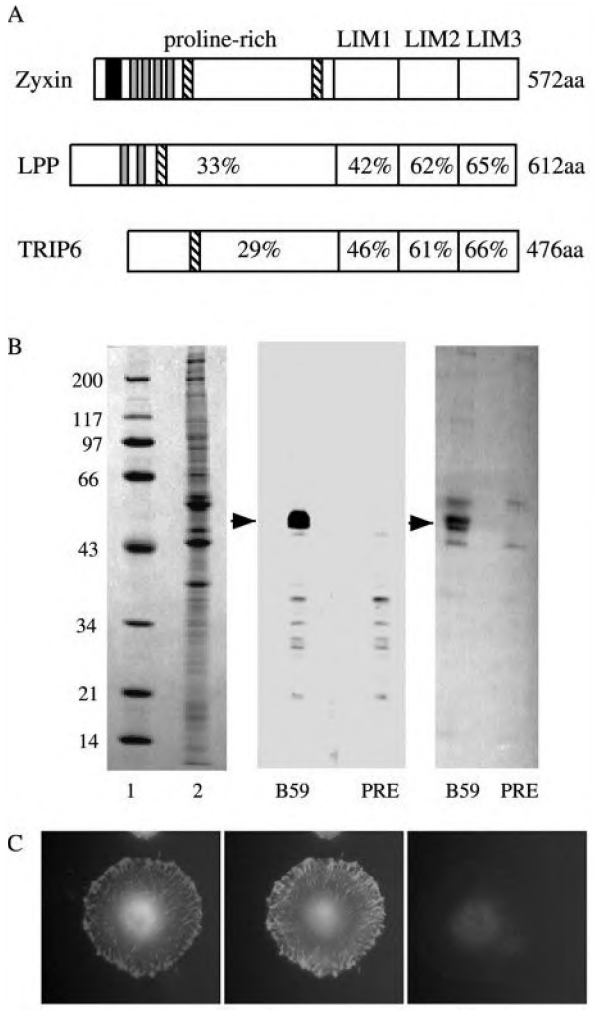

FIG. 1. *A*, schematic representation illustrating molecular structures and sequence similarity of zyxin family proteins: zyxin, LPP, and TRIP6. All zyxin family members display an NH_2-terminal proline-rich region, one or two nuclear export signal (*hatched small boxes*), and three copies of the LIM domain at their COOH termini. Zyxin and LPP contain 4 and 2 FPPPP motifs (*small gray boxes*), respectively. The FPPPP motif serves as a binding site for Mena/VASP family proteins. Zyxin also exhibits α-actinin-binding site (*black box*) within the NH_2-terminal 40 amino acid residues. The amino acid sequence of the NH_2-terminal region and each of the three LIM domains were compared individually with the sequence of zyxin and the relationship to zyxin is shown in percentage identity. *B*, characterization of the anti-peptide antibody B59 directed against TRIP6. *Left panel*, Coomassie Blue-stained gel showing molecular markers (*lane 1*) and proteins of an IMR-90 cell lysate (*lane 2*). *Middle panel*, proteins from a parallel gel were transferred to nitrocellulose membrane and probed with the anti-TRIP6 antibody (B59) and its corresponding preimmune serum (*PRE*). A protein doublet of 50 and 48 kDa is specifically recognized by the anti-TRIP6 antiserum, B59. *Right panel*, lysates prepared from [^{35}S]methionine/cysteine-labeled IMR-90 cells were used for immunoprecipitation using the anti-TRIP6 antibody (B59) and its corresponding preimmune serum (*PRE*). The immunoprecipitated proteins were resolved on a SDS-polyacrylamide gel and visualized by autoradiography. A protein doublet of 48 and 50 kDa is specifically immunoprecipitated by the anti-TRIP6 antibody, B59. *C*, localization of TRIP6 at focal adhesions. The subcellular localization of TRIP6 was determined by indirect double immunofluorescence by using an affinity-purified rabbit polyclonal antibody raised against TRIP6 (*left panel*) and a mouse monoclonal antibody against vinculin, used as a marker for focal adhesions (*middle panel*). TRIP6 is extensively co-localized with vinculin at focal adhesions. No focal adhesion staining was detected with preimmune serum (*right panel*).

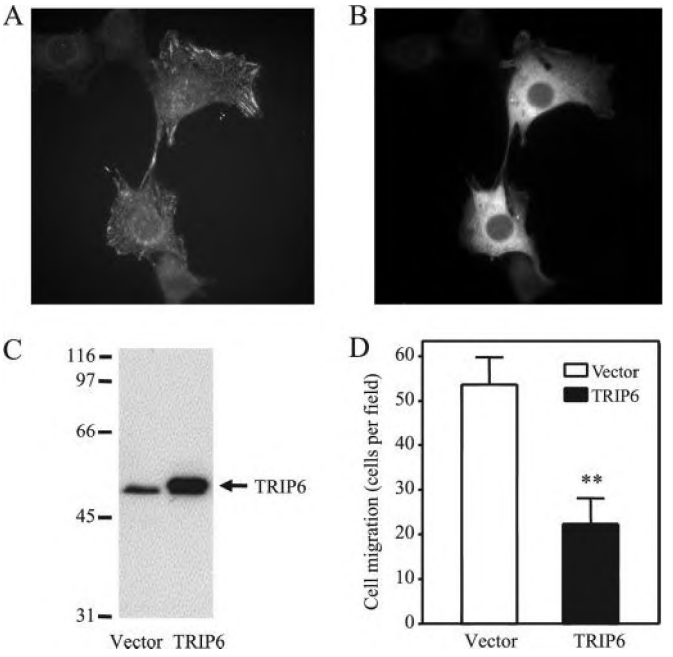

FIG. 2. **Overexpression of TRIP6 decreases cell migration.** 10T1/2 cells were transiently transfected with either empty vector or with vector containing FLAG-TRIP6 cDNA. *A*, localization of exogenous TRIP6 was detected by indirect immunofluorescence using a mouse monoclonal antibody against the FLAG epitope. *B*, transfected cells were identified by indirect immunofluorescence using a polyclonal antibody against β-galactosidase. *C*, overexpression of TRIP6 was monitored by Western blot analysis. Proteins from either vector (vector) or FLAG-TRIP6 (TRIP6) transfected cells were separated by SDS-PAGE, transferred to nitrocellulose, and probed with an anti-TRIP6 antibody. *D*, the haptotaxis migration assay was utilized to monitor cell migration. Cells were allowed to migrate for 6 h on bovine serum albumin- or fibronectin-coated membranes. The number of migrating transfected cells was measured by counting cells on the underside of the membrane that coexpressed β-galactosidase. Each determination represents the average of three individual wells and *error bars* represent the standard error of the mean. This *graph* is a representative of one of five experiments. The TRIP6-expressing cells show a statistically significant decrease in cell migration over vector-transfected cells ($p = 0.0046$) as determined by the paired Student's *t* test.

Screening for TRIP6-binding Proteins by Yeast Two-hybrid Method—To identify protein partners that might cooperate with TRIP6 to affect motility, we performed an interaction screen using the yeast two-hybrid system. The LIM region represents the most highly conserved sequence feature among the three zyxin family members (Fig. 1*A*) and LIM domains represent well characterized protein-binding sites. Therefore, in an effort to identify new interactive partners for TRIP6 that would likely be relevant for other zyxin family members as well, we focused our initial efforts on a screen for proteins that could interact with the LIM region of TRIP6. We employed a two-hybrid screen based on the activation of two reporter genes *HIS3* and *lacZ* whose expression is driven by upstream LexA DNA-binding sites.

In our initial two-hybrid screen, we tried to use the three COOH-terminal LIM domains of TRIP6. However, LexA-TRIP6LIM(1–3) alone activated reporter gene expression in yeast as assayed by measuring β-galactosidase activity (data not shown). Deletion of sequences encoding the third LIM domain of TRIP6 reduced the activation of reporter gene expression to near background, therefore we used a LexA-TRIP6LIM(1–2) fusion as the bait in our two-hybrid screen. As outlined in Fig. 3*A*, we screened ~5 million independent cDNA clones that were synthesized from day 10.5 mouse embryo mRNA by random priming. We isolated 29 HIS+ colonies at day 3.5 and an additional 45 HIS+ colonies at day 4.5 after library transformation and plating on selective medium with 45 mM 3-aminotriazole. Of the 74 HIS+ transformants isolated in the initial screen, 67 were able to activate the *lacZ* reporter

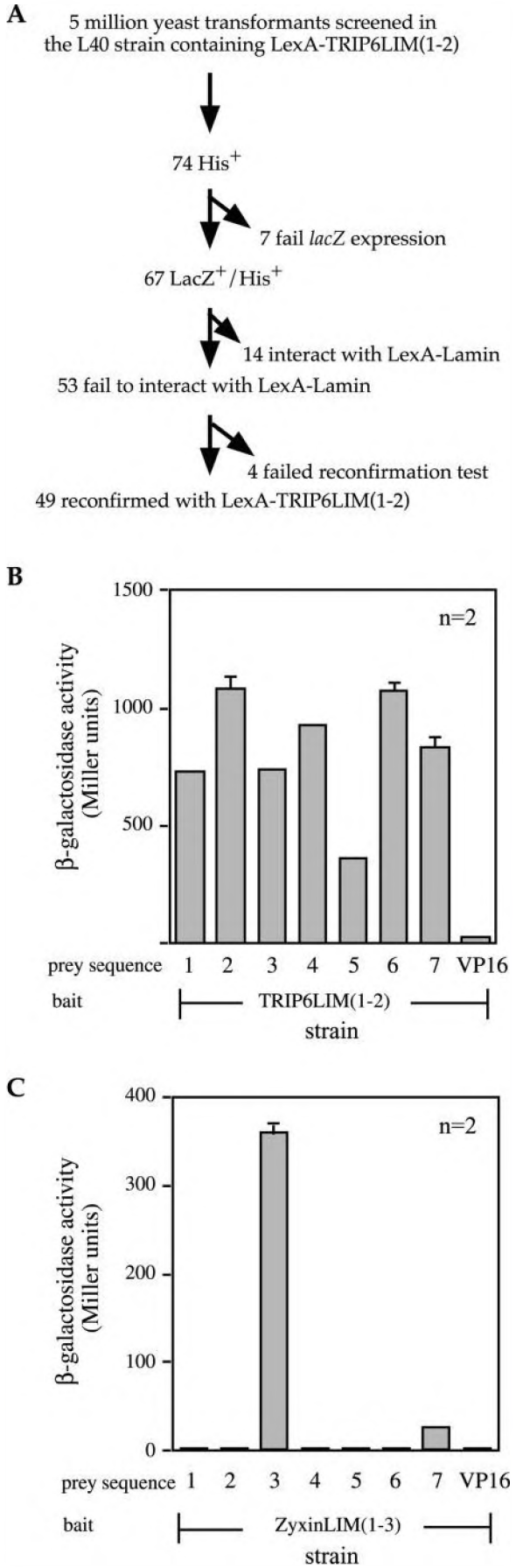

FIG. 3. *A*, the yeast two-hybrid method for identification of binding partners for the LIM regions of TRIP6 and zyxin. Schematic diagram illustrating the protocol for the isolation of sequences that specifically interact with TRIP6LIM(1–2) in yeast. *B*, relative strength of interactions between prey sequences and TRIP6LIM(1–2). β-Galactosidase activities were measured in total lysates of yeast cells containing *lacZ* reporter. The yeast cells contained bait and prey plasmids as indicated *below* the *bars*. β-Galactosidase activity by TRIP6LIM(1–2) is also shown. The prey sequences are summarized in Table I. *Error bars* indicate standard deviation. *C*, relative strength of interactions between prey sequences and zyxinLIM(1–3). β-Galactosidase activities were measured in total lysates of yeast cells containing *lacZ* reporter. The yeast cells contained bait and prey plasmids as indicated *below* the *bars*. *Error bars* indicate standard deviation.

gene expression ~20–80-fold higher than the background level of LexA-TRIP6LIM(1–2). To evaluate the specificity of the two-hybrid interactions in yeast, we eliminated the pBTM116/ADE2-TRIP6LIM(1–2) bait plasmid from the 67 HIS+/LacZ+ colonies and the resulting strains were mated to DY151 strains containing a bait plasmid encoding LexA, LexA-Lamin, or LexA-TRIP6LIM(1–2). Of the 67 prey clones isolated in the primary screen, 49 retained the ability to interact with LexA-TRIP6LIM(1–2), but did not interact with LexA or LexA-Lamin. The cDNA inserts from each of the 49 pVP16-mouse cDNA plasmids were sequenced and searched for similar sequences. All but 5 cDNA inserts represented *bona fide* open reading frames in the correct orientations for expression. Twenty-eight of the remaining 44 cDNAs were selected multiple times and shared extensive sequence similarity to previously identified coding sequences. The proteins isolated multiple times in our screen for TRIP6-binding proteins include a nuclear glycoprotein gp210 (75), a highly conserved novel ORF (accession numbers: AL031282 (human), AE003818 (*Drosophila*), U18779 (yeast), AE004170 (*Vibrio*) and U67635 (*Methanococcus*)), atrophin-1-related protein (76), CasL/HEF1 (57), tropomyosin 4 (77), synaptic GTPase activating protein (78), and a nuclear protein SON (79) (Table I). To further characterize the interactions between TRIP6LIM(1–2) and the seven prey sequences described above, we performed quantitative β-galactosidase assays. The yeast strains containing both LexA-TRIP6LIM(1–2) bait and the prey sequences show dramatically increased β-galactosidase activities relative to the strains containing LexA-TRIP6LIM(1–2) alone (Fig. 3*B*).

CasL/HEF1 Interacts with Both TRIP6 and Zyxin in Yeast—The LIM region of TRIP6 is very similar in sequence to that of zyxin. Specifically, the first and second LIM domains of TRIP6 show 46 and 61% sequence identity to the corresponding LIM domains of zyxin (Fig. 1*A*). Because of this sequence similarity, we tested whether zyxin could interact with the seven TRIP6-binding partners identified in the yeast two-hybrid screen. We used a zyxin bait construct that contains all three LIM domains of zyxin, LexA-zyxinLIM(1–3). LexA-zyxinLIM(1–3) did not exhibit the transcriptional activities by itself or in the presence of VP16 DNA-binding leader sequence (Fig. 3*C*). Interestingly, of the seven prey sequences that interact with TRIP6LIM(1–2), only CasL/HEF1 and the nuclear protein SON were able to activate *lacZ* expression with LexA-zyxinLIM(1–3) (Fig. 3*C*).

Zyxin LIM(1–2) Are Necessary and Sufficient for the CasL/HEF1 Interaction—We decided to focus first on the characterization of the interaction with CasL/HEF1 because, of the seven prey sequences isolated multiple times in our screen, it showed the greatest capacity to interact with both TRIP6 and zyxin in yeast. In addition, CasL/HEF1 has been reported to localize at focal adhesions like TRIP6 and zyxin providing further support that these interactions may be physiologically relevant. CasL/HEF1 is a "docking" protein that shows sequence and functional similarity to $p130^{Cas}$. Both CasL/HEF1 and $p130^{Cas}$ contain an NH_2-terminal SH3 domain followed by an SH2-binding substrate region and a COOH-terminal conserved region (57, 58). Previous studies have shown that CasL/

TABLE I
TRIP6-binding partners identified in a yeast two-hybrid screen

Sequence	Number of clones isolated at day		Homologues (% identity[b])	Relative strength of two-hybrid interaction with[c]		Refs.
	3.5	4.5[a]		TRIP6	Zyxin	
1	7	0	Nuclear glycoprotein gp210 (human; 91%)	++++	−	Greber *et al.* (75)
2	4	1	Novel protein similar to yeast, worm hypothetical protein (human; 98%)	++++	−	
3	4	0	CasL/HEF1 (human; 87%)	++++	++++	Law *et al.* (57)
4	0	4	Atrophin-1 related protein (human; 95%)	++++	−	Seki *et al.* (76)
5	0	3	Tropomyosin 4 (human; 95%)	++++	−	Yamawaki-Kataoka *et al.* (77)
6	0	2	Synaptic GTPase activating protein (rat; 97%)	++++	−	Kim *et al.* (78)
7	3	0	SON, DNA-binding nuclear protein	++++	+	Shimada *et al.* (79)

[a] The number of times each sequence was isolated at day 3.5 and 4.5 after library transformation was indicated.
[b] Sequence similarity to known proteins are indicated by percent identity based on blast data search.
[c] Relative strength of the interactions was measured by quantitative β-galactosidase assay. Refer to Fig. 3, *B* and *C*.

HEF1 interacts with multiple signaling components. The SH2-binding substrate region recruits a Crk family adaptor protein called Crkl upon integrin engagement and the SH3 domain interacts with focal adhesion kinase $pp125^{FAK}$ (57, 80). The COOH-terminal conserved region interacts with the v-Abl tyrosine kinase in transformed NIH3T3 cells (57). CasL/HEF1 and $p130^{Cas}$ have been suggested to play a central role in assembly and coordination of intracellular signaling components at focal adhesions (57).

We first tested which region of zyxin is required for the interaction with CasL/HEF1. We used a series of LexA fusion constructs containing sequences encoding individual or multiple LIM domains from zyxin (Fig. 4*A*) to map the sequences necessary for interaction with CasL/HEF1. Western immunoblot analysis of the yeast cell lysates using a polyclonal antibody directed against LexA showed that all the LexA-zyxinLIM fusion constructs were expressed at comparable levels (data not shown). As can be seen in Fig. 4*B*, no individual LIM domain is sufficient to support robust binding to CasL/HEF1. Rather, multiple LIM domains appear necessary, with LIM(1–2) showing greater activity than LIM(2–3).

CasL/HEF1 is a member of the Cas family that includes $p130^{Cas}$ and Efs/Sin. All three members display similar sequence and molecular structure with an NH_2-terminal SH3 domain, multiple YXXP motifs that serve as SH2 domain-binding sites, and a COOH-terminal conserved region (56–60) (Fig. 5). All of the CasL/HEF1 clones isolated in the yeast two-hybrid screen encode a part of the SH2 domain-binding region and contain 7 out of the 13 YXXP motifs present in full-length CasL/HEF1 (Fig. 5). The SH2 domain-binding substrate region of $p130^{Cas}$ contains 15 YXXP sequences and is about 55% similar to that of CasL/HEF1. Because of these structural features and the sequence similarity of $p130^{Cas}$ to CasL/HEF1, we tried to test if the substrate region of $p130^{Cas}$ could interact with the LIM regions of TRIP6 and zyxin in the yeast. However, it was not possible to test the ability of $p130^{Cas}$ to interact with TRIP6 or zyxin using the yeast two-hybrid screen because of protein instability of the VP16-$p130^{Cas}$ fusion protein and intrinsic transcriptional activity of LexA-$p130^{Cas}$ fusion proteins containing the substrate region of $p130^{Cas}$ (data not shown).

Zyxin Family Members Are Associated with $p130^{Cas}$ in Mammalian Cells—To examine the interactions between the zyxin and the Cas family members *in vivo*, we performed co-immunoprecipitation experiments with lysates from IMR-90 human fibroblasts. The anti-zyxin antibody (B38) was raised against a peptide derived from human zyxin. By Western immunoblot analysis, this antibody recognizes zyxin, which migrates at ~80 kDa. We recently determined that this antibody also recognizes the closely related zyxin family member, LPP (data not shown). Importantly, the B38 anti-zyxin antibody does not cross-react with $p130^{Cas}$ (Fig. 6*A*). As can be seen in Fig. 6*B* (*lane 1*), $p130^{Cas}$ is present in immunoprecipitates performed under nondenaturing conditions using the anti-zyxin antibody. $p130^{Cas}$ is not detected when the preimmune serum is used in these native immunoprecipitation experiments (Fig. 6*B*, *lane 2*). The recovery of $p130^{Cas}$ in the immunoprecipitate with zyxin is specific as evidenced by the fact that vinculin, another cytoskeletal protein present in the lysate is not present in the precipitated complex with zyxin and $p130^{Cas}$. Similarly, $p130^{Cas}$ is present in protein complexes recovered by native immunoprecipitation using anti-TRIP6 antibody but not control IgG (Fig. 6*C*).Vinculin is not present in either the anti-zyxin, anti-TRIP6, or control immunoprecipitates, illustrating the specificity of the recovery of $p130^{Cas}$. Importantly, all of these immunoprecipitates were performed using normal cell lysates, not ones in which proteins of interest were overexpressed. These data provide compelling evidence that $p130^{Cas}$ is associated *in vivo* with zyxin and TRIP6. We were not able to detect CasL/HEF1 in the human fibroblast cells used for these immunoprecipitation studies so it was not possible to assess the association of CasL/HEF1 with zyxin family members under these conditions.

Zyxin and $p130^{Cas}$ Are Associated in a Cell Adhesion-independent Manner—As discussed above, both zyxin and $p130^{Cas}$ are components of focal adhesions. The role of $p130^{Cas}$ in integrin-mediated signaling pathways has been extensively studied. It is reported that the tyrosine phosphorylation levels of $p130^{Cas}$ are regulated by cell adhesion to the ECM (81, 82) and some of the protein-protein interactions involving $p130^{Cas}$ are regulated by cell adhesion and tyrosine phosphorylation (32, 35). To test whether zyxin and $p130^{Cas}$ interact in an adhesion-dependent manner, we performed a co-immunoprecipitation assay using the anti-zyxin antiserum (B38) and compared the ability of zyxin to associate with $p130^{Cas}$ from the lysates of adherent *versus* detached IMR-90 fibroblasts. As shown in Fig. 7, comparable amounts of $p130^{Cas}$ are detected in the immunoprecipitates prepared from equivalent amounts of total protein derived from adherent and suspended cells. Preimmune serum fails to precipitate $p130^{Cas}$ from either adherent or suspended cells. A comparable amount of zyxin was precipitated from the lysates of adherent and suspended cells. These data suggest that the interaction between zyxin and $p130^{Cas}$ is cell adhesion-independent.

$p130^{Cas}$ Is Not Necessary for the Targeting of Zyxin to Focal Adhesions—Recently it has been determined that the LIM region of zyxin is both necessary and sufficient for targeting of zyxin to focal adhesions. Furthermore, at least two LIM domains, either LIM(1–2) or LIM(2–3), are required for focal adhesion localization of zyxin (83). Because the interaction between members of the zyxin family and the Cas family is mediated substantially by the first two LIM domains of zyxin,

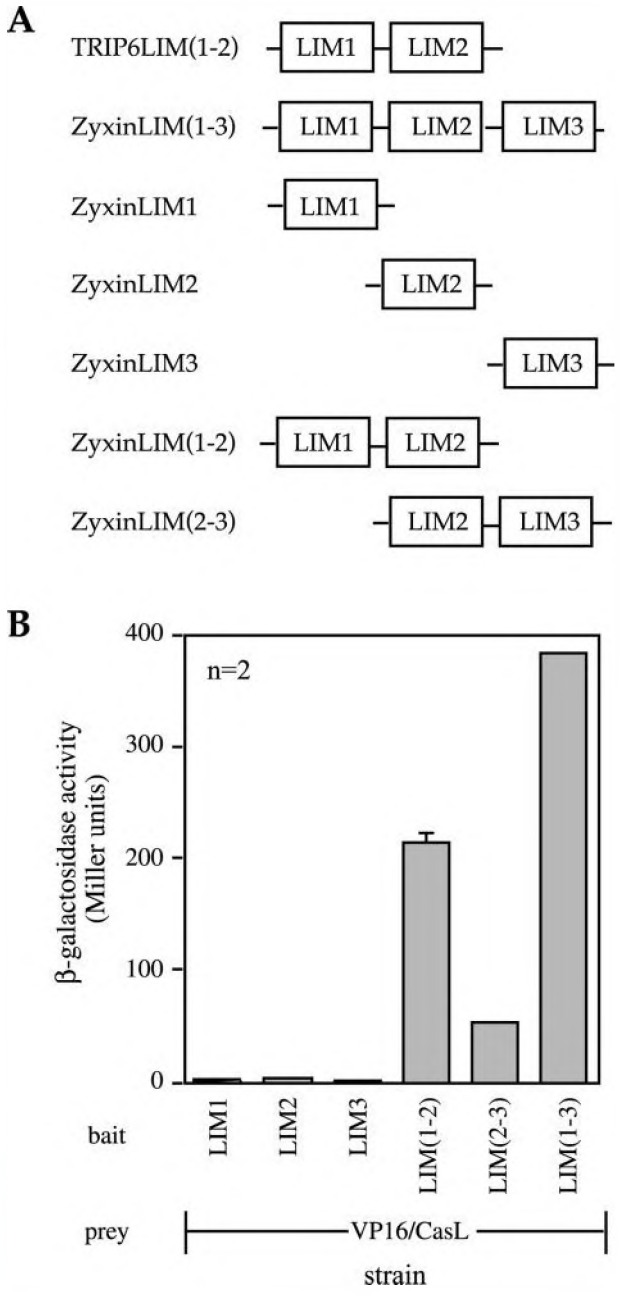

FIG. 4. *A*, schematic representation of the LIM domains of TRIP6 and zyxin fused to LexA. The TRIP6LIM(1–2) fusion construct was initially used for screening of the mouse embryo cDNA library. Prey sequences isolated in the screen were further tested for interaction with LexA-zyxinLIM(1–3) fusion. LexA fusion constructs containing one or two LIM domains of zyxin were used to determine the zyxin region that is required for the interaction with prey sequence 3 (CasL/HEF1). *B*, relative strength of the two-hybrid interactions between zyxin LIM domains and CasL was measured by quantitative β-galactosidase assay of the yeast cells. The yeast cells contained VP16/CasL and zyxin LIM fusion sequences as indicated *below* the *bars*.

we examined whether zyxin's ability to interact with $p130^{Cas}$ is critical for its recruitment to focal adhesions. To evaluate this possibility, we have compared the subcellular distributions of zyxin in mouse fibroblasts derived from wild-type and $p130^{Cas}$-null mice. During the early stages of wild-type cell spreading, zyxin is found in focal adhesions, along actin stress fibers, and in punctate structures at the leading edge (Fig. 8*A*). The punctate structures along the leading edge are focal complexes, adhesive structures that are typically found at the base of ruffling lamellipodia (84). No difference in protein composition has yet been reported between focal adhesions and focal complexes (85). However, focal complexes are morphologically distinct from focal adhesions in that focal complexes display small punctate or oblong structures. In addition, focal complexes are highly dynamic relative to focal adhesions (84). In wild-type cells, membrane protrusion is associated with the formation of zyxin-containing focal complexes at the leading edge. In $p130^{Cas}$-deficient cells, zyxin is prominently localized at focal adhesions. However, zyxin-rich focal complexes are not detected in $p130^{Cas}$-deficient cells (Fig. 8*B*). Staining with an anti-vinculin antibody likewise failed to reveal the presence of focal complexes along the leading edge in $p130^{Cas}$-deficient cells, although the cells clearly display membrane protrusion beyond focal adhesions (data not shown). This result demonstrates that $p130^{Cas}$ is not necessary for the focal adhesion targeting of zyxin. The absence of detectable focal complexes in the $p130^{Cas}$-deficient cells supports a role for Cas in assembly, maintenance, or dynamics of focal complexes.

DISCUSSION

Based on sequence similarity and overall molecular structure, we have previously identified TRIP6 as a member of the zyxin family. In this study, we report that like zyxin, endogenous TRIP6 is localized at focal adhesions. We also demonstrate that overexpression of TRIP6 results in decreased cell migration. To define possible molecular mechanisms by which TRIP6 influences cell motility, the yeast two-hybrid system was utilized to identify TRIP6-binding partners. This study revealed that both TRIP6 and zyxin are able to interact with the Cas family of focal adhesion proteins. The interactions are mediated primarily by LIM(1–2) of TRIP6 and zyxin. The LIM region is the most conserved region among zyxin family members (Fig. 1*A*). LIM(1–2) region of TRIP6, used in our two-hybrid screen, is more closely related to that of LPP than to zyxin. Specifically, LIM1 and LIM2 of TRIP6 display 61 and 77% sequence identity to the corresponding LIM domains of LPP and 46 and 61% sequence identity to those of zyxin. In fact, most of the amino acid residues of LIM(1–2) conserved between TRIP6 and zyxin are conserved in LPP. This structural feature as well as focal adhesion localization of LPP suggests that LPP may be able to interact with the Cas family members. Thus it will be of interest to test whether LPP can interact with Cas family proteins and to study the general role of the zyxin family in the regulation of Cas-mediated signaling events.

One specific function associated with the LIM region of the zyxin family is targeting to the focal adhesion. In a recent study, Nix and colleagues (83) have shown that the LIM region of zyxin is both necessary and sufficient for the targeting of zyxin to focal adhesions whereas the proline-rich NH_2-terminal region alone is targeted to the leading edge. At least two copies of the LIM domains, LIM(1–2) or LIM(2–3), are required for focal adhesion targeting (83). These results raised the possibility that focal adhesion components that interact with the LIM region of zyxin, such as $p130^{Cas}$, are good candidates to recruit zyxin and its related sequences to focal adhesions. However, zyxin's localization at focal adhesions and along the actin cytoskeleton was not affected in the $p130^{Cas}$-deficient cells. LPP also retained the ability to localize at focal adhesions (data not shown). The localization of TRIP6 in $p130^{Cas}$-deficient cells could not be tested because our anti-TRIP6 antibody fails to recognize murine TRIP6. Our results indicate that $p130^{Cas}$ is not absolutely required for focal adhesion localization of zyxin and LPP. It remains a possibility that the $p130^{Cas}$-related proteins, CasL/HEF1 and/or Efs/Sin, may compensate for the loss of $p130^{Cas}$ and play a role in targeting of zyxin family members to focal adhesions.

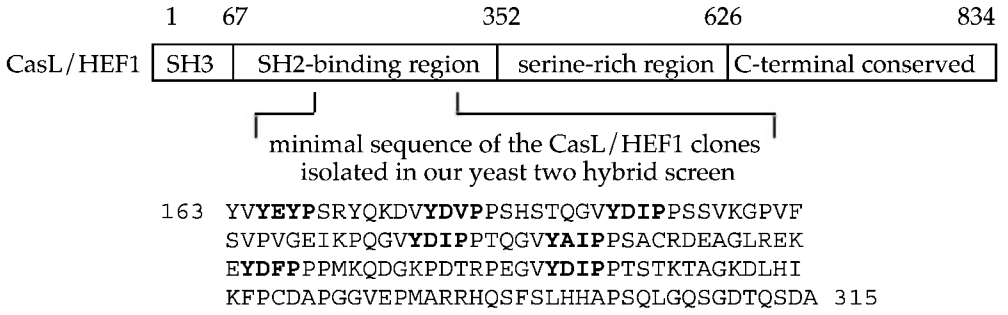

FIG. 5. **Amino acid sequence of the prey sequence 3 deduced from nucleotide sequence analysis.** The prey sequence 3 encodes a region of the SH2 domain-binding substrate region of CasL/HEF1. The region contains seven Y*XXP* motifs (in *bold*) that may be recognized by the SH2 domains when tyrosine phosphorylated. *Numbers* indicate the amino acid positions in the full-length CasL/HEF1.

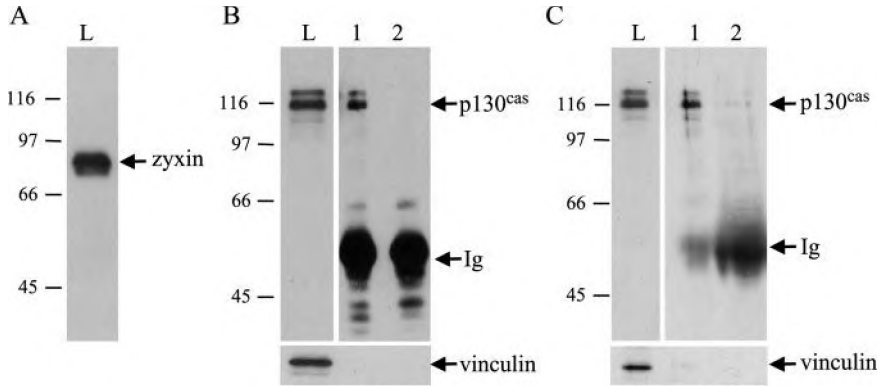

FIG. 6. **The association of zyxin and TRIP6 with p130^{Cas} in human fibroblasts.** *A*, by Western immunoblot analysis of total IMR-90 proteins (*L*), the anti-zyxin antibody recognizes zyxin/LPP at ~80 kDa and does not cross-react with p130^{Cas}. *B* and *C*, cell lysates from IMR-90 human fibroblasts contain p130^{cas} that can be detected by Western blot as a high molecular weight doublet (*panels B* and *C*, *lane L*). Such lysates were incubated with anti-zyxin antibody (*Panel B*, *lane 1*), anti-zyxin preimmune serum (*panel B*, *lane 2*), anti-TRIP6 (*panel C*, *lane 1*), or anti-TRIP6 preimmune serum (*panel C*, lane *2*) and the resulting immunoprecipitates were probed with anti-Cas antibody (*upper panels*) or anti-vinculin antibody (*lower panels*). p130^{Cas} is specifically recovered in the immunoprecipitated complex recovered with anti-zyxin and anti-TRIP6 antibodies. The absence of vinculin in the immunoprecipitates illustrates that the co-precipitation of p130^{Cas} with zyxin and TRIP6 is specific.

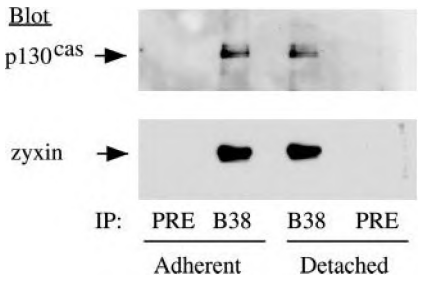

FIG. 7. **The association of zyxin and p130^{Cas} is not dependent on cell adhesion.** Cell lysates prepared from adherent or detached IMR-90 cells were immunoprecipitated with the antiserum against zyxin, *B38*, or corresponding preimmune serum (*PRE*). The immunoprecipitated proteins were analyzed with an anti-p130^{Cas} antibody or the B38 anti-zyxin antiserum.

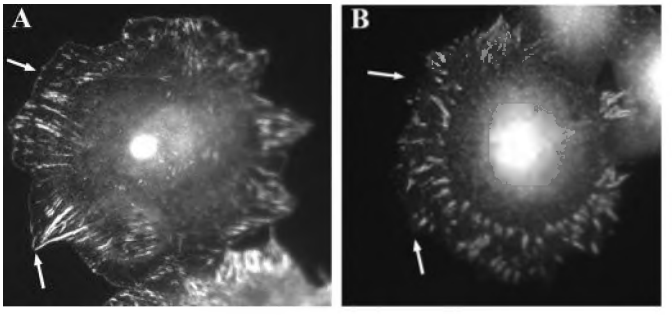

FIG. 8. **The subcellular localization of zyxin in p130^{Cas}-deficient cells.** Mouse fibroblasts derived from wild type (*A*) and p130^{Cas}-deficient (*B*) mice were plated on fibronectin-coated coverslips and the subcellular localization of zyxin was determined by an indirect immunofluorescence method. In wild-type cells, zyxin is localized at focal adhesions and focal complexes along the leading edge. However, zyxin staining at focal complexes is not detected in p130^{Cas}-deficient cells.

Although the LIM(1–2) regions of zyxin and TRIP6 bind to the substrate region of the Cas family that contains a number of tyrosine phosphorylation sites, the interaction does not seem to require tyrosine phosphorylation. A number of studies have demonstrated that tyrosine phosphorylation of Cas family proteins is enhanced upon cell adhesion to ECM (81, 82). In our study, we demonstrated that the association between zyxin and p130^{Cas} is not enhanced by cell adhesion to ECM, an observation that suggests that the association is independent of the p130^{Cas} tyrosine phosphorylation status. Furthermore, because budding yeast exhibit very low levels of tyrosine kinase activity, it is unlikely that interactions detected in yeast two-hybrid screens would be dependent on this modification (86).

The CasL/HEF1 sequence we isolated in the yeast two hybrid screen exhibits seven Y*XXP* motifs including five of seven consensus sequences for binding to the Crk SH2 domain (57). Interestingly, this result raises the possibility that the binding site for zyxin and TRIP6 on p130^{Cas} may overlap with Crk's-binding site. If so, zyxin and TRIP6 may be involved in the regulation of the Cas-Crk interaction and therefore, downstream signaling pathways. Cas-Crk association has been demonstrated to play an important role in membrane ruffling and cell migration on ECM by activating the Rac signaling pathway (62). Data presented in this report establishes that overexpression of TRIP6 inhibits cell migration. One reasonable hypothesis based on these observations is that overexpression of TRIP6 results in excessive sequestration of cellular p130^{Cas}, perhaps preventing the p130^{Cas}-Crk interaction, and blocking

downstream signaling events. Our data are consistent with the hypothesis that TRIP6 can inhibit cell migration by disrupting Cas/Crk signaling; however, other experiments will be necessary to test this model. For example, in future work, it will be important to determine if Cas/Crk/TRIP6 can co-exist in a macromolecular complex and to explore whether TRIP6 overexpression has any effect on the Cas-Crk interaction.

Focal adhesions persist in $p130^{Cas}$-deficient cells; however, by either anti-zyxin or anti-vinculin staining (data not shown), focal complex structures at the leading edge are absent. Based on this observation, $p130^{Cas}$ appears to be essential to maintain a typical ratio of focal complexes to focal adhesions. A recent study revealed that focal complex and focal adhesion formation is regulated by two distinct signaling pathways, the Rac and Rho pathways (85). Focal complex formation is initiated by activation of the Rac pathway and is independent of Rho, which plays an important role in the assembly of focal adhesions and actin stress fibers (84). Rac and Rho pathways are mutually antagonistic in focal complex and focal adhesion assembly (85). Down-regulation of Rho activity leads to the up-regulation of Rac activity and thus shifts the adhesion pattern from focal adhesions to focal complexes. In contrast, down-regulation of Rac results in the loss of focal complexes and the growth of Rho-mediated focal adhesions. Based on this mutual antagonism between the Rho and Rac pathways, the apparent absence of focal complexes at the leading edges of $p130^{Cas}$-null cells raises the possibility that $p130^{Cas}$ may play a role as a positive regulator of the Rac signaling pathway and focal complex formation. In support of this possibility, it has been demonstrated that $p130^{Cas}$-mediated cell migration requires the adaptor protein Crk (62) and the association of $p130^{Cas}$ and Crk leads to the activation of the Rac-JNK (c-Jun NH_2-terminal kinase) signaling pathway (87, 88). Thus deletion of $p130^{Cas}$ may lead to the up-regulation of Rho activity and the preferential establishment of focal adhesions. Since zyxin family members can associate directly with Cas proteins, they may cooperate with Cas family members to regulate cell adhesion and motility.

Acknowledgments—We acknowledge the expert graphics and editorial advice of Diana Lim and Jenny Jensen.

REFERENCES

1. Adams, J. C., and Watt, F. M. (1993) *Development* **117,** 1183–1198
2. Giancotti, F. G., and Ruoslahti, E. (1999) *Science* **285,** 1028–1032
3. Meredith, J. J., and Schwartz, M. A. (1997) *Trends Cell Biol.* **7,** 146–150
4. Meredith, J. E., Jr., Fazeli, B., and Schwartz, M. A. (1993) *Mol. Biol. Cell* **4,** 953–961
5. Frisch, S. M., and Francis, H. (1994) *J. Cell Biol.* **124,** 619–626
6. Aplin, A. E., Howe, A., Alahari, S. K., and Juliano, R. L. (1998) *Pharmacol. Rev.* **50,** 197–263
7. Zhu, X., and Assoian, R. K. (1995) *Mol. Biol. Cell* **6,** 273–282
8. Yamada, K. M., and Miyamoto, S. (1995) *Curr. Opin. Cell Biol.* **7,** 681–689
9. Sastry, S. K., and Horwitz, A. F. (1993) *Curr. Opin. Cell Biol.* **5,** 819–831
10. Clark, E. A., and Brugge, J. S. (1995) *Science* **268,** 233–239
11. Kumar, C. C. (1998) *Oncogene* **17,** 1365–1373
12. Juliano, R. L., and Haskill, S. (1993) *J. Cell Biol.* **120,** 577–585
13. Schwartz, M. A., Schaller, M. D., and Ginsberg, M. H. (1995) *Annu. Rev. Cell Dev. Biol.* **11,** 549–599
14. Lewis, J. M., Baskaran, R., Taagepera, S., Schwartz, M. A., and Wang, J. Y. (1996) *Proc. Natl. Acad. Sci. U. S. A.* **93,** 15174–15179
15. Lewis, J. M., and Schwartz, M. A. (1998) *J. Biol. Chem.* **273,** 14225–14230
16. Vuori, K., and Ruoslahti, E. (1993) *J. Biol. Chem.* **268,** 21459–21462
17. Chen, Q., Kinch, M. S., Lin, T. H., Burridge, K., and Juliano, R. L. (1994) *J. Biol. Chem.* **269,** 26602–26605
18. Defilippi, P., Venturino, M., Gulino, D., Duperray, A., Boquet, P., Fiorentini, C., Volpe, G., Palmieri, M., Silengo, L., and Tarone, G. (1997) *J. Biol. Chem.* **272,** 21726–21734
19. King, W. G., Mattaliano, M. D., Chan, T. O., Tsichlis, P. N., and Brugge, J. S. (1997) *Mol. Cell. Biol.* **17,** 4406–4418
20. Angers-Loustau, A., Cote, J. F., Charest, A., Dowbenko, D., Spencer, S., Lasky, L. A., and Tremblay, M. L. (1999) *J. Cell Biol.* **144,** 1019–1031
21. Garton, A. J., and Tonks, N. K. (1999) *J. Biol. Chem.* **274,** 3811–3818
22. Garton, A. J., Flint, A. J., and Tonks, N. K. (1996) *Mol. Cell. Biol.* **16,** 6408–6418
23. Liu, F., Hill, D. E., and Chernoff, J. (1996) *J. Biol. Chem.* **271,** 31290–31295
24. Tamura, M., Gu, J., Danen, E. H., Takino, T., Miyamoto, S., and Yamada, K. M. (1999) *J. Biol. Chem.* **274,** 20693–20703
25. Mainiero, F., Murgia, C., Wary, K. K., Curatola, A. M., Pepe, A., Blumemberg, M., Westwick, J. K., Der, C. J., and Giancotti, F. G. (1997) *EMBO J.* **16,** 2365–2375
26. Barry, S. T., Flinn, H. M., Humphries, M. J., Critchley, D. R., and Ridley, A. J. (1997) *Cell Adhes. Commun.* **4,** 387–398
27. Clark, E. A., King, W. G., Brugge, J. S., Symons, M., and Hynes, R. O. (1998) *J. Cell Biol.* **142,** 573–586
28. Ren, X. D., Kiosses, W. B., and Schwartz, M. A. (1999) *EMBO J.* **18,** 578–585
29. Renshaw, M. W., Toksoz, D., and Schwartz, M. A. (1996) *J. Biol. Chem.* **271,** 21691–21694
30. Schlaepfer, D. D., Hanks, S. K., Hunter, T., and van der Geer, P. (1994) *Nature* **372,** 786–791
31. Schaller, M. D., and Parsons, J. T. (1995) *Mol. Cell. Biol.* **15,** 2635–2645
32. Vuori, K., Hirai, H., Aizawa, S., and Ruoslahti, E. (1996) *Mol. Cell. Biol.* **16,** 2606–2613
33. Burnham, M. R., Harte, M. T., Richardson, A., Parsons, J. T., and Bouton, A. H. (1996) *Oncogene* **12,** 2467–2472
34. Harte, M. T., Hildebrand, J. D., Burnham, M. R., Bouton, A. H., and Parsons, J. T. (1996) *J. Biol. Chem.* **271,** 13649–13655
35. Polte, T. R., and Hanks, S. K. (1995) *Proc. Natl. Acad. Sci. U. S. A.* **92,** 10678–10682
36. Beckerle, M. C. (1997) *Bioessays* **19,** 949–957
37. Crawford, A. W., and Beckerle, M. C. (1991) *J. Biol. Chem.* **266,** 5847–5853
38. Macalma, T., Otte, J., Hensler, M. E., Bockholt, S. M., Louis, H. A., Kalff-Suske, M., Grzeschik, K. H., von der Ahe, D., and Beckerle, M. C. (1996) *J. Biol. Chem.* **271,** 31470–31478
39. Nix, D. A., and Beckerle, M. C. (1997) *J. Cell Biol.* **138,** 1139–1147
40. Sadler, I., Crawford, A. W., Michelsen, J. W., and Beckerle, M. C. (1992) *J. Cell Biol.* **119,** 1573–1587
41. Golsteyn, R. M., Beckerle, M. C., Koay, T., and Friederich, E. (1997) *J. Cell Sci.* **110,** 1893–1906
42. Niebuhr, K., Ebel, F., Frank, R., Reinhard, M., Domann, E., Carl, U. D., Walter, U., Gertler, F. B., Wehland, J., and Chakraborty, T. (1997) *EMBO J.* **16,** 5433–5444
43. Laurent, V., Loisel, T. P., Harbeck, B., Wehman, A., Grobe, L., Jockusch, B. M., Wehland, J., Gertler, F. B., and Carlier, M. F. (1999) *J. Cell Biol.* **144,** 1245–1258
44. Reinhard, M., Jouvenal, K., Tripier, D., and Walter, U. (1995) *Proc. Natl. Acad. Sci. U. S. A.* **92,** 7956–7960
45. Crawford, A. W., Michelsen, J. W., and Beckerle, M. C. (1992) *J. Cell Biol.* **116,** 1381–1393
46. Drees, B. E., Andrews, K. M., and Beckerle, M. C. (1999) *J. Cell Biol.* **147,** 1549–1560
47. Reinhard, M., Zumbrunn, J., Jaquemar, D., Kuhn, M., Walter, U., and Trueb, B. (1999) *J. Biol. Chem.* **274,** 13410–13418
48. Drees, B., Friederich, E., Fradelizi, J., Louvard, D., Beckerle, M. C., and Golsteyn, R. M. (2000) *J. Biol. Chem.* **275,** 22503–22511
49. Fradelizi, J., Noireaux, V., Plastino, J., Menichi, B., Louvard, D., Sykes, C., Golsteyn, R. M., and Friederich, E. (2001) *Nat. Cell Biol.* **3,** 699–707
50. Schmeichel, K. L., and Beckerle, M. C. (1994) *Cell* **79,** 211–219
51. Arber, S., Halder, G., and Caroni, P. (1994) *Cell* **79,** 221–231
52. Hirota, T., Morisaki, T., Nishiyama, Y., Marumoto, T., Tada, K., Hara, T., Masuko, N., Inagaki, M., Hatakeyama, K., and Saya, H. (2000) *J. Cell Biol.* **149,** 1073–1086
53. Lee, J. W., Choi, H. S., Gyuris, J., Brent, R., and Moore, D. D. (1995) *Mol. Endocrinol.* **9,** 243–254
54. Yi, J., and Beckerle, M. C. (1998) *Genomics* **49,** 314–316
55. Zhao, M. K., Wang, Y., Murphy, K., Yi, J., Beckerle, M. C., and Gilmore, T. D. (1999) *Gene Expr.* **8,** 207–217
56. Sakai, R., Iwamatsu, A., Hirano, N., Ogawa, S., Tanaka, T., Mano, H., Yazaki, Y., and Hirai, H. (1994) *EMBO J.* **13,** 3748–3756
57. Law, S. F., Estojak, J., Wang, B., Mysliwiec, T., Kruh, G., and Golemis, E. A. (1996) *Mol. Cell. Biol.* **16,** 3327–3337
58. Minegishi, M., Tachibana, K., Sato, T., Iwata, S., Nojima, Y., and Morimoto, C. (1996) *J. Exp. Med.* **184,** 1365–1375
59. Ishino, M., Ohba, T., Sasaki, H., and Sasaki, T. (1995) *Oncogene* **11,** 2331–2338
60. Alexandropoulos, K., and Baltimore, D. (1996) *Genes Dev.* **10,** 1341–1355
61. Cary, L. A., Han, D. C., Polte, T. R., Hanks, S. K., and Guan, J. L. (1998) *J. Cell Biol.* **140,** 211–221
62. Klemke, R. L., Leng, J., Molander, R., Brooks, P. C., Vuori, K., and Cheresh, D. A. (1998) *J. Cell Biol.* **140,** 961–972
63. Honda, H., Oda, H., Nakamoto, T., Honda, Z., Sakai, R., Suzuki, T., Saito, T., Nakamura, K., Nakao, K., Ishikawa, T., Katsuki, M., Yazaki, Y., and Hirai, H. (1998) *Nat. Genet.* **19,** 361–365
64. Honda, H., Nakamoto, T., Sakai, R., and Hirai, H. (1999) *Biochem. Biophys. Res. Commun.* **262,** 25–30
65. O'Neill, G. M., Fashena, S. J., and Golemis, E. A. (2000) *Trends Cell Biol.* **10,** 111–119
66. Harlow, A., and Lane, D. (1988) in *Antibodies: A Laboratory Manual*, pp. 313–315, Cold Spring Harbor Laboratory, Cold Spring Harbor, NY
67. Pomies, P., Louis, H. A., and Beckerle, M. C. (1997) *J. Cell Biol.* **139,** 157–168
68. Polte, T. R., and Hanks, S. K. (1997) *J. Biol. Chem.* **272,** 5501–5509
69. Beckerle, M. C. (1986) *J. Cell Biol.* **103,** 1679–1687
70. Hollenberg, S. M., Sternglanz, R., Cheng, P. F., and Weintraub, H. (1995) *Mol. Cell. Biol.* **15,** 3813–3822
71. Thomas, B. J., and Rothstein, R. (1989) *Cell* **56,** 619–630
72. McCright, B., and Virshup, D. M. (1995) *J. Biol. Chem.* **270,** 26123–26128
73. Wang, Y., Dooher, J. E., Koedood Zhao, M., and Gilmore, T. D. (1999) *Gene (Amst.)* **234,** 403–409
74. Petit, M. M., Fradelizi, J., Golsteyn, R. M., Ayoubi, T. A., Menichi, B., Louvard, D., Van De Ven, W. J., and Friederich, E. (2000) *Mol. Biol. Cell* **11,** 117–129

75. Greber, U. F., Senior, A., and Gerace, L. (1990) *EMBO J.* **9,** 1495–1502
76. Seki, N., Ohira, M., Nagase, T., Ishikawa, K., Miyajima, N., Nakajima, D., Nomura, N., and Ohara, O. (1997) *DNA Res.* **4,** 345–349
77. Yamawaki-Kataoka, Y., and Helfman, D. M. (1987) *J. Biol. Chem.* **262,** 10791–10800
78. Kim, J. H., Liao, D., Lau, L. F., and Huganir, R. L. (1998) *Neuron* **20,** 683–691
79. Shimada, K., Harata, M., and Mizuno, S. (1997) *J. Cell Sci.* **110,** 3031–3041
80. Astier, A., Manie, S. N., Law, S. F., Canty, T., Haghayghi, N., Druker, B. J., Salgia, R., Golemis, E. A., and Freedman, A. S. (1997) *Leuk. Lymphoma* **28,** 65–72
81. Petch, L. A., Bockholt, S. M., Bouton, A., Parsons, J. T., and Burridge, K. (1995) *J. Cell Sci.* **108,** 1371–1379
82. Nojima, Y., Morino, N., Mimura, T., Hamasaki, K., Furuya, H., Sakai, R., Sato, T., Tachibana, K., Morimoto, C., Yazaki, Y., and Hirai, H. (1995) *J. Biol. Chem.* **270,** 15398–15402
83. Nix, D. A., Fradelizi, J., Bockholt, S., Menichi, B., Louvard, D., Friederich, E., and Beckerle, M. C. (2001) *J. Biol. Chem.* **276,** 34759–34767
84. Nobes, C. D., and Hall, A. (1995) *Cell* **81,** 53–62
85. Rottner, K., Hall, A., and Small, J. V. (1999) *Curr. Biol.* **9,** 640–648
86. Keegan, K., and Cooper, J. A. (1996) *Oncogene* **12,** 1537–1544
87. Dolfi, F., Garcia-Guzman, M., Ojaniemi, M., Nakamura, H., Matsuda, M., and Vuori, K. (1998) *Proc. Natl. Acad. Sci. U. S. A.* **95,** 15394–15399
88. Kiyokawa, E., Hashimoto, Y., Kobayashi, S., Sugimura, H., Kurata, T., and Matsuda, M. (1998) *Genes Dev.* **12,** 3331–3336